Aerospace Science and Technology ••• (••••) •••–•••

Contents lists available at ScienceDirect

Aerospace Science and Technology

www.elsevier.com/locate/aescte

Dynamic stall control on flapping wing airfoils

Wolfgang Geissler [a,*], Berend G. van der Wall [b]

[a] German Aerospace Center, Institute of Aerodynamics and Flow Technology, Göttingen, Germany
[b] German Aerospace Center, Institute of Flight Systems, Braunschweig, Germany

A R T I C L E I N F O

Article history:
Received 2 March 2016
Received in revised form 14 November 2016
Accepted 7 December 2016
Available online xxxx

Keywords:
Flapping wing aerodynamic
Dynamic stall
Dynamic stall control
MAV-aerodynamics
Bird and insect flight

A B S T R A C T

Flapping wing efficiency is limited by flow separation effects. The time dependent development of a leading edge vortex (LEV) during rapid pitch-up motion of a retreating helicopter rotor blade is known as dynamic stall vortex. Movement of this vortex along the airfoil upper surface first increases lift but later the vortex lifts off the airfoil surface causing strong drag rise, severe nose-down pitching moments, and possibly negative aerodynamic damping. Very similar effects can be observed on flapping airfoils and wings experiencing combined plunging (heaving) motion and pitching motion. With increasing plunge amplitude the flow on the flapping wing starts to separate and concentrated dynamic stall vortices may develop on both upper and lower wing surfaces. Under these conditions it is shown that wing propulsion efficiency is considerably reduced. Recent investigations of dynamic stall control have shown that a strong vortex may be avoided by appropriate airfoil deformation. It will be shown in the present paper that with dynamic airfoil deformation the propulsion efficiency can be improved considerably. The validity of the numerical calculations is first tested against existing data from literature.

1. Introduction

Flapping wing aerodynamics have been investigated very intensively in recent years [1–3]. The aim is to learn from natural flyers and to make this knowledge applicable to small size artificial flight vehicles known as Micro Air Vehicles (MAV) with a maximum dimension of ∼15 cm and a further reduction to NAV (Nano Air Vehicles) with dimensions less than 7.5 cm. These flight vehicles mimic small size birds and insects with high frequency flapping wings operating at moderate to small Reynolds numbers ($Re < 40000$) where the flow is definitely laminar.

The flow about helicopter rotor blades in forward flight condition has some common features compared to natural flyers: The flow is also highly unsteady, concentrated vortices may occur at the airfoil leading edge (LEV) and finally separated flow limits the flight envelope. On helicopter blades, as well as on flapping wings, concentrated vortices may develop at the leading edge and move along the upper or lower surface of the airfoil. These vortices, together with successive airfoil stall, are assumed to limit the flight envelope of a helicopter and also limit the amount of forward thrust and propulsion efficiency of a flapping wing.

Numerical results for a NACA 0012 airfoil section in pure plunging motion have been discussed in [4] utilizing a Navier–Stokes code. Flow separation limits thrust and propulsion efficiency at relatively small effective incidences depending on plunge amplitude, frequency, Mach and Reynolds numbers. The results are considerable improved if pitching motion is added with a certain phase shift between pitch and plunge.

In [5] it has been shown that the efficiency reaches an optimum when pitch leads plunge around a phase shift of 90°. Under these conditions the flow does not show concentrated dynamic stall vortices which are clearly present at phase shifts much less or larger than 90°. In [6] the combination of flapping and pitching rotor blades has been applied to the concept of a “flapping propulsion rotor” with the aim to avoid a tail rotor.

When an airfoil undergoes pitch and plunge motions a considerable number of parameters are involved: Amplitudes, frequency, and phase shift angles between plunge and pitch. Several researchers have tried to optimize flow cases with respect to maximum thrust and efficiency, [7,8]. The latter research shows that under optimized conditions a leading edge vortex does not show up over most parts of the oscillation cycle.

It is well known that bird and insect wings have flexible structures which may deform both span wise as well as chord wise. A chord wise dynamic shape deformation has been measured on dragon fly wings, [2]; it has been shown that a positive (nose down) camber develops during the down stroke motion of the wing followed by a negative camber during up stroke. In [3] several methods have been discussed to solve the aero-elastic prob-

* Corresponding author.
E-mail address: wolfgang.geissler@dlr.de (W. Geissler).

http://dx.doi.org/10.1016/j.ast.2016.12.008
1270-9638/

Nomenclature

a_∞	Speed of sound .... m/s
c	Airfoil chord .... m
c_D	Drag coefficient, $c_D = c_{Dp} + c_{Df}$
c_{Df}	Drag coefficient due to surface friction
c_{Dp}	Drag coefficient due to air pressure
c_L	Lift coefficient
$c_{L\alpha}$	Lift curve slope, $c_{L\alpha} = 2\pi$
c_P	Power coefficient
C_P	Mean power coefficient
c_T	Thrust coefficient, $c_T = -c_D$
C_T	Mean thrust coefficient
f	Frequency of oscillation .... Hz
h	Non-dimensional plunging amplitude, referenced to chord, $h = z/c$
Ma	Mach number, $Ma = U_\infty/a_\infty$
$\overline{P}$	Mean value of section power per unit span .... (N m/s)/m
Q	Pitching moment about pitch axis per unit span .... N m/m
Re	Reynolds number, $Re = U_\infty c/\nu$
t	Time .... s
T_p	Time of an oscillation period, $T_p = 2\pi/\omega$ .... s
$\overline{T}$	Non-dimensional time, $\overline{T} = tU_\infty/c$
$\overline{T}_p$	Non-dimensional time of an oscillation period, $\overline{T}_p = 2\pi/\omega^*$
T	Normalized time, $T = \overline{T}/\overline{T}_p$
U_∞	Free-stream velocity .... m/s
V_h	Normal velocity induced by plunging motion .... m/s
x, z	Horizontal and vertical coordinate .... m
x_{pf}, z_{pf}	Location of flex-center .... m
X, Z	Horizontal and vertical section force per unit span .... N/m
$\overline{X}$	Mean value of horizontal section force per unit span .... N/m
α	Mean pitch angle .... deg
Θ	Effective incidence, $\Theta = \alpha + \Theta_p + \Theta_h$
Θ_h	Incidence induced by plunging motion, $\Theta_h = -\tan^{-1}(V_p/U_\infty)$ .... deg
Θ_{h0}	Amplitude of incidence induced by plunging motion, $\Theta_{h0} = -\tan^{-1}(\omega^* h)$ .... deg
Θ_p	Incidence of pitching motion .... deg
Θ_{p0}	Amplitude of pitching incidence .... deg
η	Propulsion efficiency, $\eta = C_T/C_P$
ν	Kinematic viscosity .... m^2/s
ρ	Air density .... kg/m^3
ϕ	Phase shift between pitch and plunge .... deg
ψ	Nose-droop angle .... deg
$\Delta\psi$	Amplitude of nose-droop angle .... deg
ω	Rotational frequency of airfoil oscillation, $\omega = 2\pi f$ .... rad/s
ω^*	Reduced frequency, $\omega^* = \omega c/U_\infty$

lem, i.e. combine both aerodynamic and structural dynamic forces to determine the final shape of the wing.

2. Motivation

The present numerical study is restricted to 2D airfoils oscillating in prescribed harmonic motions.

A lot of effort has been made recently to apply and improve numerical codes based on the full Navier–Stokes equations to solve problems of unsteady flows with separation i.e. dynamic stall problems on helicopter rotor blades. It has also been shown both numerically and experimentally, [9–12], that dynamic stall can be controlled either by dynamic airfoil deformation (dynamic drooping) or by passive control devices (leading edge modifications). It is indicated in [12] that during rapid up-stroke motion severe vorticity peaks develop within a very small instant of space and time. Vorticity can no longer follow the airfoil surface. It breaks off into the flow, and is rolling up to form concentrated vortices. These common features occur during dynamic stall on a helicopter airfoil at pitching motion, [12].

Fig. 1 shows hysteresis loops for lift and pitching motion on a typical helicopter airfoil section during deep dynamic stall. The experimental curves (red) are representing 160 consecutive cycles; it is observed that during up stroke and at the end of down stroke all curves are on top of each other: in these regions the flow is attached. As soon as the flow separates close to the maximum incidence ($\alpha = 18.9°$) the curves are spreading over a wider range. The numerical results obtained with the present code [14] fit reasonable well to the experimental data. Two calculations are presented: Fully turbulent results (blue) and results with transition (green). In the nonseparated areas only small differences are present; at stall onset and during the start of down stroke however severe deviations are detected: with transition the fit to the experimental data is considerably improved compared to the result obtained with fully turbulent calculation.

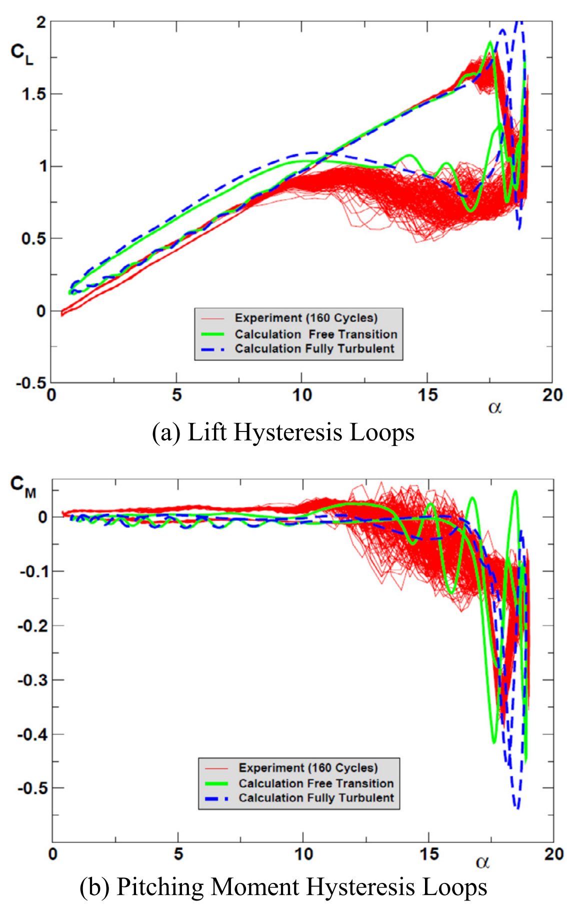

Fig. 1. Numerical OA209 helicopter airfoil at deep dynamic stall (from [12]); $\alpha = 9.8° \pm 9.1°$, $Ma = 0.3$, $Re = 1.15 \cdot 10^6$, $\omega^* = 0.1$. (For interpretation of the colors in this figure, the reader is referred to the web version of this article.)

Please cite this article in press as: W. Geissler, B.G. van der Wall, Dynamic stall control on flapping wing airfoils, Aerosp. Sci. Technol. (2016), http://dx.doi.org/10.1016/j.ast.2016.12.008